Theranostic Agents

DOI: 10.1002/anie.201008286

Gold-Nanoshelled Microcapsules: A Theranostic Agent for Ultrasound Contrast Imaging and Photothermal Therapy**

Hengte Ke, Jinrui Wang, Zhifei Dai, Yushen Jin, Enze Qu, Zhanwen Xing, Caixin Guo, Xiuli Yue, and Jibin Liu*

The term theranostics, which is derived from "diagnostics" and "therapy", refers to a treatment strategy that combines a diagnostic test and a specific therapy based on the test results.[1] This integration of diagnostic imaging capability with therapy is critical in addressing the challenges of cancer heterogeneity and adaptation. Therefore, theranostic agents have received a great deal of recent research interest in cancer diagnosis and treatment.[2]

Among all the diagnostic imaging techniques, ultrasound imaging has a unique advantage because of its features of real-time, low-cost, high safety, and ease of incorporation into portable devices.[3] With the use of ultrasound contrast agents (UCAs), the resolution and sensitivity of clinical ultrasound imaging have been greatly improved.[4] Microcapsules composed of poly(lactic acid) (PLA), which has outstanding biocompatibility and biodegradability, show good ultrasound contrast-enhancing capabilities and other advantages: they have good mechanical strength and are thus stable, they can load either hydrophilic or hydrophobic species or both, and they are surface-charged and have functional groups on the surface so that they could be easily modified to introduce further practical features.[5]

Gold nanostructures exhibit good biocompatibility as well as excellent optical and electronic properties, thus allowing use in biological and medical applications.[6] Gold nanoshells have a spherical dielectric core particle surrounded by a thin nanoscale gold shell. By controlling the thickness of the gold shell and the diameter of the core, the plasmon resonance and the resulting optical absorption of gold nanoshells can be tuned to the near-infrared (NIR) region, where the absorption of human tissues is minimal and penetration is optimal.[7] On the other hand, the strong optical absorption of nanoshells can rapidly increase the local temperature under NIR irradiation.[8] Therefore, the gold nanoshells can be used as photoabsorbers for remote NIR photothermal ablation therapy.

Lasers and photoabsorbers such as gold nanostructures are used to carry out cancer treatment in photothermal therapy. However, the location and size of cancers must be identified before therapy, the treatment procedure needs to be monitored in real time during therapy, and the effectiveness has to be assessed after therapy. Contrast-enhanced ultrasound imaging could be the technique of choice to address these tasks. Therefore, the development of gold-nanoshell-based UCAs could operate as a multifunctional theranostic agent for imaging-guided photothermal therapy.

We have developed a novel multifunctional theranostic agent based on gold-nanoshelled microcapsules (GNS-MCs) by electrostatic adsorption of gold nanoparticles as seeds onto the polymeric microcapsule surfaces, followed by the formation of gold nanoshells by using a surface seeding method (Figure 1). The polymeric microcapsules were generated from PLA and polyvinyl alcohol (PVA) materials by employing the water-in-oil-in-water (W/O/W) double-emulsion method,[5] and were negatively charged with a zeta potential of about −25 mV. Upon exposure to positively charged poly(allyl-

[*] H. T. Ke, Prof. Z. F. Dai, Y. S. Jin, Dr. Z. W. Xing, Dr. C. X. Guo, Prof. X. L. Yue
Nanomedicine and Biosensor Laboratory, School of Sciences
State Key Laboratory of Urban Water Resources and Environment
Harbin Institute of Technology, Harbin, 150001 (P.R. China)
Fax: (+86) 451-8640-3192
E-mail: zhifei.dai@hit.edu.cn
Homepage: http://nanobio.hit.edu.cn/
Prof. J. R. Wang, E. Z. Qu
Department of Ultrasonography
Peking University Third Hospital, Beijing 100083 (P.R. China)
Prof. J. B. Liu
Ultrasound Research and Education Institute,
Thomas Jefferson University, Philadelphia, PA 19107 (USA)

[**] This research was financially supported by the National Natural Science Foundation of China (NSFC-30970829, 30672001), the National High Technology Research and Development Program of China (no. 2007AA03Z316), and the Cultivation Fund of the Key Scientific and Technical Innovation Project, Ministry of Education of China (no. 707021).

Supporting information for this article is available on the WWW under http://dx.doi.org/10.1002/anie.201008286.

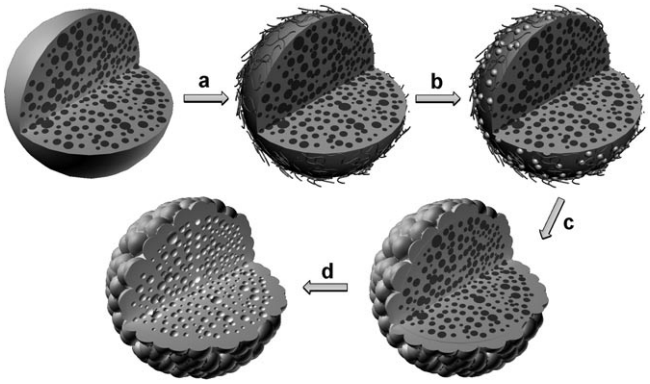

Figure 1. Fabrication process of gold-nanoshelled microcapsules: a) electrostatic adsorption of PAH onto microcapsules generated by the W/O/W double-emulsion method; b) deposition of gold nanoparticles onto PAH-coated microcapsules; c) formation of gold nanoshells by the surface-seeding method; d) lyophilization to sublimate the encapsulated water in the inner aqueous phase of the microcapsules to produce small hollow spaces.

amine hydrochloride) (PAH), the surface charge was converted into about +2 mV. On the contrary, when citrate-stabilized gold nanoparticles (GNPs, with a zeta potential of about −12 mV) were adsorbed onto the surface of the PAH-coated microcapsules, a zeta potential of around −26 mV was measured, thus indicating the successful alternating deposition of PAH and GNPs onto the surface of microcapsules. Then, the attached gold nanoseeds were used to nucleate the growth of a gold coating around the microcapsule surface by a seeding procedure. $NH_2OH{\cdot}HCl$ was used to reduce the gold precursor $HAuCl_4$ to bulk metal without the nucleation of new particles; all the added gold was incorporated into larger particles that were deposited on the surface of the capsules.[9] As the gold nanoparticles grew large enough to aggregate, nanoshells formed around the microcapsule surface. In our synthesis, the polymeric microcapsules provided a dielectric interface for shifting the plasmon resonance of the gold nanoshells to the NIR wavelength region.[10] After lyophilization, the encapsulated water in the inner aqueous phase of the microcapsules was sublimated to leave a small hollow space that could provide a basis for the ultrasound-responsive properties. The gold shells on the outer surface can be heated by NIR lasers as photoabsorbers for photothermal ablation therapy, thus making the GNS-MC composites a novel theranostic agent.

The typical morphology of the blank microcapsules (MCs) and GNS-MCs was analyzed by SEM (Figure 2). The bare MCs showed a well-defined spherical shape with a smooth surface, and the diameter ranged from hundreds of nanometers to several micrometers (Figure 2a). After reduction of $HAuCl_4$ to form gold nanoshells, the obtained GNS-MCs maintained their spherical shape and developed slightly rough surfaces (Figure 2b). The aggregated gold particles on the surface of the microcapsules could be clearly observed in the magnified SEM images (Figure 2c,d), thus confirming the successful fabrication of gold nanoshells.

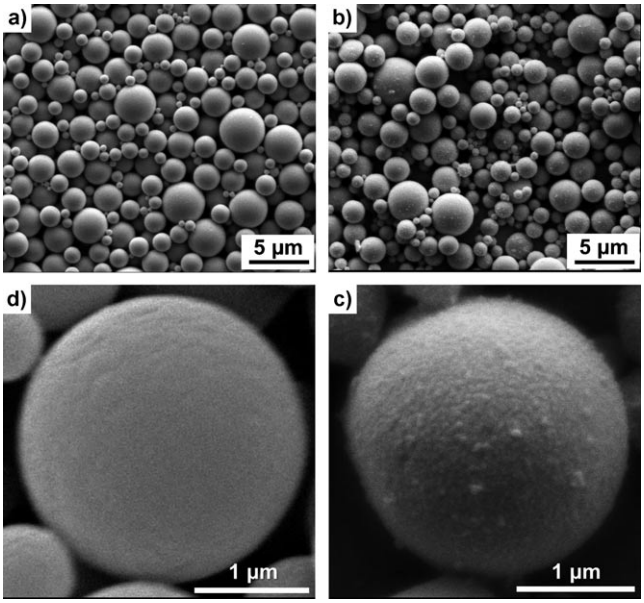

Figure 2. SEM micrographs of bare MCs (a) and GNS-MCs (b); (c) and (d) are expansions of the images in (a) and (b), respectively.

To determine the component elements of the resulting composites, energy dispersive X-ray spectroscopy (EDS) spectra of blank MCs and GNS-MCs on an Al plate without gold sputtering were acquired (see Figure S1 in the Supporting Information). The spectrum of GNS-MCs showed the presence of 14.78% elemental gold, thus suggesting that the gold shells were formed on the MCs. The microcapsules could be imaged by SEM without gold sputtering as the gold-nanoshell covering made their conductivity sufficiently high (Figure S2).

UV/Vis spectra and TEM images of samples at different preparation stages, including blank MCs, GNP-MCs, and GNS-MCs were collected (Figure 3). The extinction spectrum

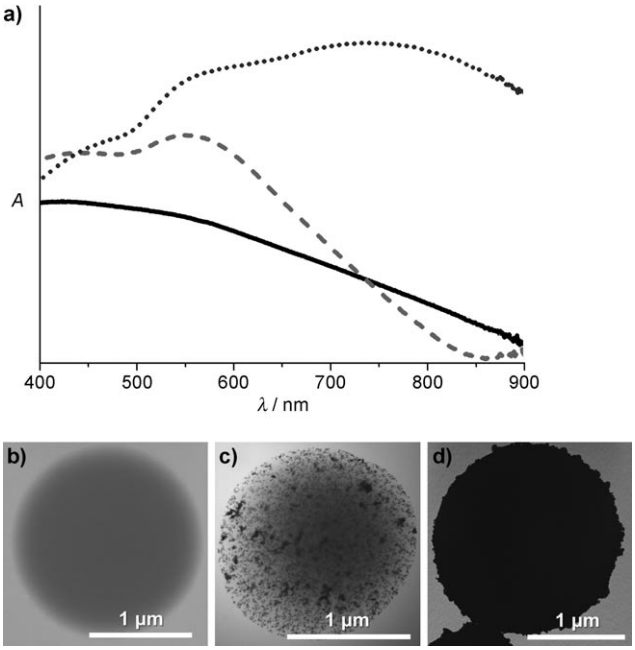

Figure 3. a) UV/Vis spectra (—— MCs; ----- GNP-MCs; ••••• GNS-MCs) and TEM images of gold-nanoshelled microcapsules at different stages of the fabrication process: b) MCs, c) GNP-MCs, and d) GNS-MCs.

of the MCs exhibited no obvious peak in the range from 400 nm to 900 nm (Figure 3a), which can be attributed to the light scattering of submicrometer/micrometer capsules.[11] The TEM image of blank MCs (Figure 3b) displayed a homogeneous spherical shape. After treatment with the gold colloid, densely distributed dark spots could be seen on the surface of the capsules (Figure 3c), thus indicating the successful deposition of gold nanoparticles, which made the intensity of the plasmon resonance around 500–600 nm increase to form a peak. The seeding process made the attached gold nanoparticles grow large enough to cluster and form a dense shell. The resulting GNS-MCs had rough edges and seemed to be much more compact (Figure 3d), and the UV/Vis spectrum showed a new broad peak ranging from 650 to 900 nm and a shoulder peak around 500–650 nm. The red-shift and

broadening of the plasmon resonance peak of the gold species could be attributed to the wider size distribution and aggregation of the gold nanoparticles on the capsule surface.[11] The broad absorbance between 650 and 900 nm suggests that the GNS-MCs would be suitable for photothermal therapy with light in the NIR region, as there is minimal absorption of light of this wavelength in tissues.

One of the essential features of UCAs is the size of the microcapsules. The agent must be smaller than 7 μm in diameter in order to cross pulmonary capillaries to produce the systemic enhancement.[4] The size distributions of blank MCs and GNS-MCs were measured by using static light scattering (SLS; Figure S3). The average sizes were measured to be (1.87 ± 1.08) μm and (2.32 ± 1.07) μm for blank MCs and GNS-MCs, respectively. More than 99% of GNS-MCs had diameters less than 7 μm, and thus these microcapsules meet the requirement as a UCA for clinical application.

The most crucial feature required for the composite agents to act as UCAs is that they exhibit excellent echogenic properties. The basic contrast-enhancing principle of UCAs is that the backscattering echo intensity is proportional to the change in acoustic impedance between the tissues and the injected agents.[4a] Thus, the acoustic enhancement of obtained GNS-MCs was evaluated both in vitro and in vivo. A previously described procedure[12] was applied to in vitro ultrasound contrast imaging. A suspension of GNS-MCs was injected into a latex tube containing circulating saline. Ultrasound contrast images with and without agent injection in both pulse-inversed harmonic imaging (PIHI) mode and conventional B mode are shown in Figure 4a,b. In the presence of GNS-MCs, obvious grayscale imaging enhancement in the PIHI contrast mode was seen within the lumen of the tube, thus suggesting the good contrast-enhancing ability of the GNS-MCs.

A further evaluation of the ultrasound contrast behavior of GNS-MCs was carried out using New Zealand white rabbits. PIHI contrast mode (with mechanical index, MI = 0.42) and conventional B-mode sonograms before and after administration of GNS-MCs are shown in Figure 4c,d. Excellent enhancements of rabbit kidney images were clearly seen in a few seconds after bolus intravenous injection of the agent, thus suggesting that GNS-MCs were able to traverse pulmonary capillaries to achieve systemic enhancement and is consistent with the results of in vitro ultrasonography. The contrast enhancement lasted more than 5 minutes, which is long enough to satisfy the clinical requirements. The vital signs of the rabbits were unaffected during the entire procedure, and no arrhythmia and other side effects were observed, thus indicating the composite agents showed no evidence of acute toxicity.

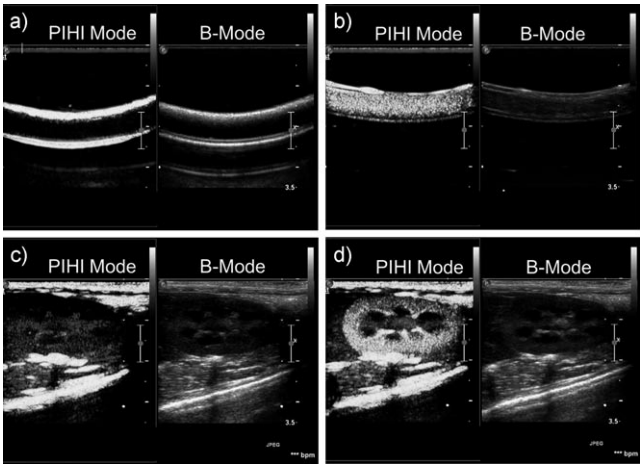

Figure 4. In vitro ultrasound contrast-enhanced images in a latex tube a) without and b) with GNS-MCs; in vivo ultrasonograms in the rabbit right kidney c) pre- and d) post-administration of GNS-MCs. Both PIHI (MI = 0.42) and conventional B-mode images are shown.

An important feature of gold nanoshells is the NIR light-induced thermal effect, which could be used for the selective treatment of solid tumors.[7] To investigate temperature elevation induced by NIR laser irradiation in the presence of GNS-MCs, different concentrations of the nanoshells (with same total volume of 4.0 mL) in a quartz cell were exposed to a continuous-wave fiber-coupled diode laser with a center wavelength of 808 nm and output power of 2 W. Figure 5a shows the temperature of samples under irradiation recorded at 10-second intervals. The temperature rose with increasing exposure time. For an aqueous dispersion of GNS-MCs, the temperature elevation of 25, 15, 12, and 5 °C was achieved under the irradiation of NIR laser for 10 minutes at concentrations of 0.5, 0.3, 0.15, and 0.05 mg mL^{-1}, respectively. In contrast, no significant temperature change was observed when deionized water was exposed to the laser light, thus verifying the excellent photothermal efficiency of GNS-MCs. At an initial temperature of 30 °C, samples with concentrations greater than 0.15 mg mL^{-1} can be easily heated up to above 42 °C, which is sufficient to kill tumor cells.[13] These data indicate that GNS-MCs could act as an efficient photothermal mediator.

To evaluate the localized tumor photohyperthermic effect of GNS-MCs, HeLa cells (human cervical carcinoma cell lines) cultured in six-well plates were incubated with the GNS-MCs for 1 hour, followed by illumination with an NIR laser (808 nm and 8 W cm^{-2} for 10 min). When the cancer cells are exposed to higher temperatures, intracellular proteins could be denatured to inhibit normal cellular growth and proliferation.[14] After variable combination treatment with agents and lasers, fluorescent cell staining for assessment of cell viability was carried out with the nonfluorescent cell permeable dye calcein AM; this dye can be converted into calcein, which has a strong green fluorescence, when hydrolyzed by intracellular esterases in live cells.[15] Under an inverted fluorescence microscope (Figure 5b), a dark region was observed in the presence of both the agent and laser (Figure 5b, image D) that arises from the NIR laser-induced hyperthermic effect on cancer cells. Cells outside of the illumination spot exhibited the green fluorescence of calcein, which indicated the survival of HeLa cells. In contrast, other samples (Figure 5b, images A–C) showed a vivid green color in the entire well, thus suggesting that exposure of cancer cells to either GNS-MCs or a high-intensity NIR laser alone did not compromise cell viability. The dark region in Figure 5b (image D) matched the irradiated area, thus indicating that

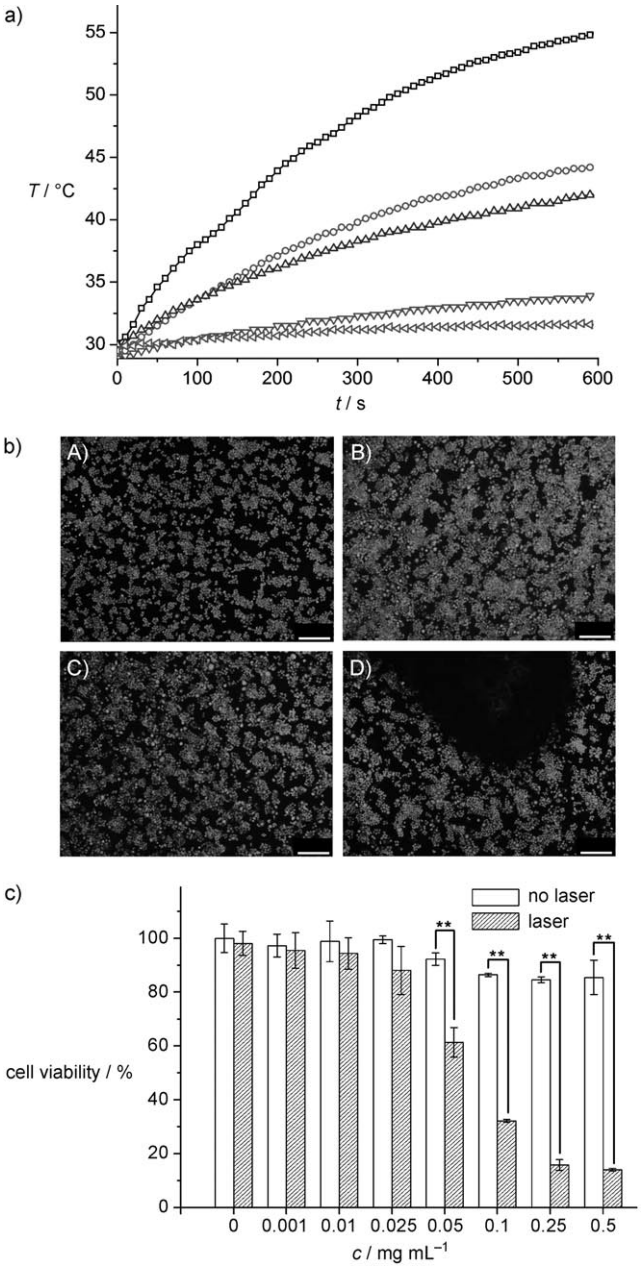

Figure 5. a) Temperatures of GNS-MCs agent at different concentrations (◁ 0 (deionized water), ▽ 0.05, △ 0.15, ○ 0.3, □ 0.5 mg mL^{-1}) under NIR laser irradiation (808 nm, 2 W) measured every 10 s with a digital thermometer over a period of 10 min. b) Fluorescence microscopy images of HeLa cells with different treatments stained with calcein AM: A) no agent and no laser irradiation; B) laser irradiation only; C) agent only; D) with both agent and laser irradiation. Note that the dark area represents the region of killed HeLa cells. (Scale bars: 500 μm; GNS-MCs agent concentration: 0.3 mg mL^{-1}; NIR laser: 808 nm, 8 W cm^{-2}, 10 min.) c) HeLa cell viabilities at different dosages of GNS-MCs (0, 0.001, 0.01, 0.025, 0.05, 0.1, 0.25, and 0.5 mg mL^{-1}) with or without laser irradiation (808 nm, 4 W cm^{-2}, 10 min). Data shown as mean ± SD, $n = 3$; $^{**}p < 0.01$ and $^{*}p < 0.05$.

GNS-MCs will cause cancer cells to die through photothermal effects only under NIR laser irradiation.

We further evaluated the photothermal cytotoxicity of GNS-MCs with and without laser irradiation on HeLa cells using a MTT (3-(4,5-dimethylthiazol-2-yl)-2,5-diphenyltetrazolium bromide) assay. As described above, the size of GNS-MCs ranged from hundreds of nanometers to several micrometers, and thus they are too large to penetrate into cytoplasma. Therefore, GNS-MCs were incubated with HeLa cells to allow adhesion to the cell membrane for laser-induced thermal therapy. Figure 5c shows that HeLa cells treated with GNS-MCs without laser illumination remained more than 80% viable at concentrations ranging from 0.001 to 0.5 mg mL^{-1}, thus suggesting that GNS-MCs had little impact on cell survival even at higher concentrations. However, when simultaneously treated with GNS-MCs and laser irradiation (808 nm, 4 W cm^{-2}, 10 min), the cell viabilities significantly decreased as the concentration increased. At lower concentrations (0.001–0.025 mg mL^{-1}), no obvious photohyperthermia effect was observed and over 80% of cancer cells remained alive. In contrast, at higher concentrations (0.05–0.5 mg mL^{-1}), the cell viabilities decreased rapidly with laser irradiation. In particular, only less than 20% of HeLa cells remained viable when they were incubated with more than 0.25 mg mL^{-1} of GNS-MCs under NIR irradiation, thus indicating a significant photothermal therapeutic effect. These experimental findings demonstrated that the combination of GNS-MCs and NIR laser illumination can effectively kill the tumor cells in vitro, and thus GNS-MCs could act as a photoabsorber for photothermal tumor therapy.

GNS-MCs can be used as a theranostic agent for simultaneous diagnosis and treatment of tumors by utilizing their enhanced ultrasound imaging capabilities and photothermal effects. By administration of this novel theranostic agent, ultrasound contrast imaging can be applied to identify the size and location of the tumor, and then, under real-time ultrasound guidance and monitoring, targeted NIR laser-induced photothermal therapy could be carried out based on the diagnostic imaging results, thus avoiding the damage of normal tissues. Finally, after the treatment procedure, the effectiveness of the therapy could be evaluated by UCAs-assisted diagnosis to determine whether or not to carry out further treatment. This diagnosis may significantly shorten the treatment time, simplify the procedure, and make the treatment more efficient.

In conclusion, we successfully constructed GNS-MCs composed of ultrasound-responsive polymeric microcapsules for systemic contrast-enhanced ultrasound imaging diagnosis, and NIR-absorbing gold nanoshells on the surface for remote photohyperthermia. HeLa cells incubated with GNS-MCs in vitro can be killed photothermally by exposure to NIR light. Meanwhile, GNS-MCs can still maintain adequate acoustic properties that are required to act as an ultrasound contrast agent. Thus, the dual-functional nano/micro composites hold a great potential for ultrasound-guided photothermal tumor therapy. This simple and highly efficient theranostic agent would remarkably improve the methodologies for cancer diagnosis and therapy.

Received: December 31, 2010
Published online: February 25, 2011

Keywords: contrast imaging · gold · microcapsules · photothermal therapy · theranostic agents

[1] S. Warner, *Scientist* **2004**, *18*, 38 – 39.
[2] a) B. Sumer, J. M. Gao, *Nanomedicine* **2008**, *3*, 137 – 140; b) A. Louie, *Chem. Rev.* **2010**, *110*, 3146 – 3195.
[3] Z. Liu, F. Kiessling, J. Gätjens, *J. Nanomater.* **2010**, 894303.
[4] a) Z. W. Xing, H. T. Ke, J. R. Wang, B. Zhao, X. L. Yue, Z. F. Dai, J. B. Liu, *Acta Biomater.* **2010**, *6*, 3542 – 3549; b) Z. W. Xing, J. R. Wang, H. T. Ke, B. Zhao, X. L. Yue, Z. F. Dai, J. B. Liu, *Nanotechnology* **2010**, *21*, 145607.
[5] a) W. J. Cui, J. Z. Bei, S. G. Wang, G. Zhi, Y. Y. Zhao, X. S. Zhou, H. W. Zhang, Y. Xu, *J. Biomed. Mater. Res. B* **2005**, *73*, 171 – 178; b) D. M. El-Sherif, J. D. Lathia, N. T. Le, M. A. Wheatley, *J. Biomed. Mater. Res. Part A* **2004**, *68 A*, 71 – 78.
[6] Y. T. Lim, O. O. Park, H. T. Jung, *J. Colloid Interface Sci.* **2003**, *263*, 449 – 453.
[7] L. R. Hirsch, R. J. Stafford, J. A. Bankson, S. R. Sershen, B. Rivera, R. E. Price, J. D. Hazle, N. J. Halas, J. L. West, *Proc. Natl. Acad. Sci. USA* **2003**, *100*, 13549 – 13554.
[8] J. Yang, J. Lee, J. Kang, S. J. Oh, H. J. Ko, J. H. Son, K. Lee, J. S. Suh, Y. M. Huh, S. Haam, *Adv. Mater.* **2009**, *21*, 4339 – 4342.
[9] K. R. Brown, M. J. Natan, *Langmuir* **1998**, *14*, 726 – 728.
[10] X. J. Ji, R. P. Shao, A. M. Elliott, R. J. Stafford, E. Esparza-Coss, J. A. Bankson, G. Liang, Z. P. Luo, K. Park, J. T. Markert, C. Li, *J. Phys. Chem. C* **2007**, *111*, 6245 – 6251.
[11] T. H. Ji, V. G. Lirtsman, Y. Avny, D. Davidov, *Adv. Mater.* **2001**, *13*, 1253 – 1256.
[12] H. T. Ke, Z. W. Xing, B. Zhao, J. R. Wang, J. B. Liu, C. X. Guo, X. L. Yue, S. Q. Liu, Z. Y. Tang, Z. F. Dai, *Nanotechnology* **2009**, *20*, 425105.
[13] G. M. Hahn, J. Braun, I. Har-Kedar, *Proc. Natl. Acad. Sci. USA* **1975**, *72*, 937 – 940.
[14] D. Hanahan, R. A. Weinberg, *Cell* **2000**, *100*, 57 – 70.
[15] F. Braut-Boucher, J. Pichon, P. Rat, M. Adolphe, M. Aubery, J. Font, *J. Immunol. Methods* **1995**, *178*, 41 – 51.

